Amplitude and timing of the Laschamp geomagnetic dipole low from the global atmospheric 10 Be overproduction: Contribution of authigenic 10 Be/ 9 Be ratios in west equatorial Pacific sediments

L L Ménabréaz, Didier Bourles, Nicolas Thouveny

Amplitude and timing of the Laschamp geomagnetic dipole low from the global atmospheric ^{10}Be overproduction: contribution of authigenic $^{10}Be/^{9}Be$ ratios in West Equatorial Pacific sediments.

L. Ménabréaz[1], D.L. Bourlès*, and N. Thouveny*.*

* Aix-Marseille Université, CNRS, IRD, CEREGE UM34, 13545 Aix-en-Provence Cedex 04, France.

[1] Corresponding author : menabreaz@cerege.fr

Abstract

Authigenic $^{10}Be/^{9}Be$ ratios were measured along a sediment core collected in the West Equatorial Pacific in order to reconstruct cosmogenic ^{10}Be production variations near the equator, where the geomagnetic modulation is maximum. From 60 to 20 ka, the single significant ^{10}Be production impulse recorded at 41 ka results from the geomagnetic dipole low that triggered the Laschamp excursion. No significant ^{10}Be overproduction signature is recorded at the age of the Mono Lake excursion (~34 ka). A compilation of authigenic $^{10}Be/^{9}Be$ records obtained from sediments was averaged over a 1 ka window and compared with the 1 ka-averaged ^{10}Be flux record of Greenland ice cores. Their remarkable similarity demonstrates that the ^{10}Be production is globally modulated by geomagnetic dipole variations and redistributed by atmosphere dynamics. After calibration using absolute values of the virtual dipole moment drawn from paleomagnetic database, the authigenic $^{10}Be/^{9}Be$ stack allows reconstructing the geomagnetic dipole moment variations over the 20-50 ka time interval. Between 48 ka and 41 ka, the dipole moment collapsed at a rate of -1.5 x 10^{22} $A.m^{2}.ka^{-1}$, which will be an interesting criterion for the assessment of the loss rate of the historical field and the comparison of dipole moment loss prior to excursions and reversals. After a 2 ka duration of the minimum dipole moment (~1 x 10^{22} $A.m^{2}$), a slow increase started at 39 ka, progressively reaching 5 x 10^{22} $A.m^{2}$ at 20 ka. The absence of a significant dipole moment drop at 34 ka, the age of the Mono lake excursion, suggests that the duration and amplitude of the dipole weakening cannot be compared with that of the Laschamp. This study provides a reliable basis to model the production of radiocarbon and *in-situ* cosmogenic nuclides and to improve the calibration of these dating methods.

1. Introduction

The understanding of past and present geomagnetic field behaviour depends on the accuracy and precision of proxy records of geomagnetic field magnitude and direction. Since the last geomagnetic reversal (780 ka ago), the geomagnetic dipole moment appears to have been affected by repeated drops, which generate large directional variations of the geomagnetic vector field [e.g. *Thouveny et al.,* 2008; *Channell et al.,* 2009]. The interpreted global character of these geomagnetic instabilities however strongly depends on the geographic distribution of available paleomagnetic records and on the recording materials (sediments or volcanic rocks), which influence the reliability of the recorded phenomena (amplitude and duration). This is illustrated by the ongoing debate over the occurrence of one or two dipole lows / excursions during the 30-45 ka interval: Laschamp at ~41 ka and possibly Mono Lake at ~33 ka.

Quasi-reversed magnetizations recorded in Laschamp and Olby lava flows, (Massif central, France) provided the first evidence of a past transient reversed state of the geomagnetic field [*Bonhommet and Babkine,* 1967]. The first dating by *Bonhommet and Zahringer* [1969] using K/Ar methods performed on whole rock led to an age determination between 8 and 20 ka. After almost four decades of geochronologic investigations using K–Ar, thermoluminescence, $^{40}Ar/^{39}Ar$ and ^{230}Th–^{238}U methods [e.g. *Bonhommet and Zähringer*, 1969; *Condomines*, 1980; *Hall and York*, 1978; *Gillot et al.*, 1979; *Chauvin et al.*, 1989; *Plenier et al.*, 2007], the most reliable radiometric age datasets finally led to concordant ages of 40.4±2.0 ka [*Guillou et al.*, 2004] and 40.7±1.0

ka BP [*Singer et al.,* 2009]. Meanwhile, the Laschamp excursion has been identified worldwide as a large amplitude swing of the magnetization vectors, and/or as a dramatic paleointensity low in lava flows (e.g. *Kristjansson and Gudmundsson,* 1980; *Roperch et al.,* 1988; *Levi et al.,* 1990; *Mochizuki et al.,* 2006; *Cassata et al.,* 2008] and sediments [e.g. *Thouveny and Creer,* 1992; *Vlag et al.,* 1996; *Lund et al.,* 2005; *Channell,* 2006]. These studies thus established the global extension of the geomagnetic anomaly and mark it as the major geomagnetic crisis to have occurred over the last 50 ka.

In contrast with the Laschamp case, the occurrence and/or the age of the Mono Lake (ML) excursion/dipole moment low remain controversial. *Denham and Cox* [1971], while seeking a record of the Laschamp excursion at Mono Lake (California), detected excursional paleomagnetic directions in sedimentary layers of the Wilson Creek formation. These layers were initially radiocarbon dated at ~24 ka, i.e. at an age older than the age attributed at that time to the Laschamp excursion [*Bonhommet and Zahringer*, 1969]. The ML excursion was thus considered as distinct from the Laschamp excursion. It was later described in other North-Western American lacustrine sections [e.g. *Negrini et al.,* 1984; *Liddicoat et al*., 1992; *Coe and Liddicoat*, 1994; *Hanna and Verosub*, 1989] as well as North Atlantic sediments [e.g. *Novaczyk and Knies*, 2000; *Channell*, 2006]. The age of the excursion in the Mono Lake sediment sequence has since been revised from ~24 ka [*Denham and Cox,* 1971] to ~32 – 34 ka [*Negrini et al*., 2000; *Benson et al.*, 2003; *Zic et al.* 2002]. This is, however, still subject to debate. Indeed, ^{14}C ages obtained on lacustrine carbonates and $^{40}Ar/^{39}Ar$ ages of sanidine crystals from the Wilson Creek Formation which range from 38 to 41 ka suggest, on the contrary, that the ML excursion should be assigned to the Laschamp excursion [*Kent et al.*, 2002]. The correlation of the Mono Lake RPI stack [*Zimmerman et al.*, 2006] with the GLOPIS record of *Laj et al.* [2004] supports this attribution.

Marine sediment relative paleointensity (RPI) records however, often display two successive significant RPI lows attributed to the Laschamp and Mono Lake excursions [*Nowaczyk and Knies*, 2000; *Laj et al*., 2000, 2004; *Channel et al*., 2006; *Lund et al*., 2006]. The Mono Lake RPI low is recorded at ~34.7 ka according to the correlation of the sedimentary paleoclimatic proxies with oxygen isotopes records from Greenland [GICC05 age model; *NGRIP dating group 2006*, and references therein]. Volcanic records of the Mono Lake excursion were also retrieved from New Zealand [*Shibuya et al.*, 1992; *Mochizuki et al*., 2004, 2006, 2007; *Cassata et al.*, 2008 ; *Cassidy and Hill*, 2009], Hawaii [*Laj et al*., 2002; *Teanby et al.*, 2002] and the Canary Islands [*Kissel et al.*, 2011]. The case of the Mono Lake excursion, therefore, remains controversial. Both its age and the amplitude of dipole moment reduction remain uncertain.

Deciphering the amplitude and timing of dipole moment lows can be performed using methods independent from rock- and paleomagnetism, such as those based on cosmogenic nuclide production recorded in sediments and ice cores. Meteoric Beryllium-10 (^{10}Be, half-life: 1.387 ± 0.012 Ma [*Chmeleff et al.*, 2010; *Korschinek et al.*, 2010]) is produced through nucleonic cascades in the atmosphere which result from nuclear interactions between the Galactic Cosmic Rays (GCR) and the Oxygen and Nitrogen atmospheric targets. Proportional to the flux of the highly energetic charged particles constituting the GCR, the ^{10}Be production rate is mainly modulated over multi-millennial time scales by the variability of the magnetospheric shielding dominated by the geomagnetic dipole. In appropriate archives, records of ^{10}Be production rates thus provide proxies of the geomagnetic dipole moment variations [e.g. *Lal,* 1988]. Independent from paleomagnetic methods, this approach is particularly well suited to confirm or invalidate the worldwide character of reported paleomagnetic features. Early works by *Elsasser et al.* [1956] and *Lal* [1988] allowed establishing an inverse relationship between the globally integrated ^{10}Be atmospheric production and the dipole moment magnitude. During the last decades, this relationship has been broadly confirmed using numerical simulations based on purely physical models [*Masarik and Beer,* 1999, 2009; *Wagner et al.*, 2000b], and experimentally supported by changes of ^{10}Be depositional fluxes in ice sheets [e.g. *Muscheler et al.*, 2005] and in marine sediment [e.g. *Robinson et al.,* 1995; *Frank*, 2000; *Carcaillet et al.,* 2003, 2004a; *Christl et al*., 2003] records.

Cosmogenic nuclide production records over the time interval spanning the Laschamp and Mono Lake excursions are provided by ^{10}Be and ^{36}Cl deposition flux in polar ice [e.g *Raisbeck et al*., 1992; *Finkel and Nishiizumi*, 1997; *Yiou et al.*, 1997; *Wagner et al.,* 2000 a, b; *Muscheler et al.*, 2005] and by marine sediments using $^{230}Th_{xs}$-normalized ^{10}Be fluxes [e.g *Frank et al.*, 1997; *Christl et al.*, 2010]. Authigenic ^{10}Be/^{9}Be records recently obtained from marine sediments [e.g. *Carcaillet et al.,* 2004a, b; *Leduc et al*., 2006; *Ménabréaz et al.*, 2011] encourage further studies in other regions, especially at low latitude, where the modulation of ^{10}Be production rates by the geomagnetic dipole is maximum.

2. Environmental setting and sediment description of core MD05-2920.

The studied core MD05-2920 (36.67 m long; 2.51°S, 144.32°E; 1848 m water depth) was retrieved with a giant piston corer during the MD148-PECTEN Cruise aboard the RV/Marion Dufresne in 2005 [*Beaufort et al.*, 2005]. The coring site is located on the north coast of Papua New Guinea, in the Bismarck Sea, at ~100 km off the Sepik and Ramu Rivers estuaries (Figure 1.A). These large rivers and their tributaries drain through erodible volcanic and igneous rock formations distributed along a steep topographic profile (the altitude of these "central mountains" is > 4000 m).

The regional climate is dominated by the Asian-Australian monsoon system [*Webster et al.*, 1998; *Wang et al.*, 2003]. The sediment discharge from rivers draining the north slope of the island of New Guinea [*Milliman et al.*, 1999] is thus very considerable. This area is characterized by a very narrow continental shelf (< 5 km), incised principally by the Sepik submarine canyon extending from the river mouth to water-depths greater than 1000m [*Cresswell*, 2000]. After the vertical divergence of the surface plume at the head of the canyon, the Sepik sediments disperse along two distinct routes [*Kineke et al.*, 2000]: much of the sediment is transported down the canyon via near-bottom hyperpycnal flows, while a surface plume, driven by the New Guinean Coastal Current, transports fine sediments eastward (during the NW monsoon) and westward (during the SE monsoon) along the shelf and slope. Evidence of intermediate turbid layers also suggests distal transport along isopycnal surfaces [*Kineke et al.*, 2000]. However, the wet conditions throughout the year limit aeolian particle transport to this area, contrarily to contributions from the river inputs [*Kawahata et al.*, 2000]. This depositional setting leads to sedimentation rates on the order of tens of centimeters per ka [*Beaufort et al.*, 2005].

The MD05-2920 sequence presents good stratigraphic preservation and is mainly composed of homogeneous (non-laminated) greyish olive clay, with dispersed foraminifers and occasional black lenses of organic matter [*Beaufort et al.*, 2005]. The proportion of the terrigeneous fraction in MD05-2920 core top sediments is ~70%, and that of the carbonate fraction is ~25% [*Tachikawa et al.*, 2011].

The sedimentary elemental composition as determined by X-ray fluorescence analyses [Tachikawa et al., 2011] does not present a clear glacial-interglacial variability, which implies that glacial conditions have a limited influence on the hydrological cycle, which is rather linked to the intertropical convergence zone.

3. Methodology

3.1 Transport correction:

^{10}Be concentration in marine sediments is the result of superimposed contributions. First, it depends on the atmospheric ^{10}Be flux entering the ocean and reflecting its production rate in the atmosphere. ^{10}Be is primarily produced in the stratosphere: this proportion was estimated at 67% by *Lal and Peters* [1967], and at 56% by *Masarik and Beer* [1999]. Once produced, the particle-reactive ^{10}Be set onto aerosols is integrated to the hydrological cycle and removed from the atmospheric reservoir on a yearly time-scale. *Baroni et al.* [2011] calculated a ^{10}Be atmospheric residence time of ~3 years which is a combination of a tropospheric residence time of approximately one week and a stratospheric residence time that could be as long as 6 years. This estimation is slightly higher than previous ones [*Beer et al.*, 1990; *Raisbeck et al.*, 1981], and suggests, according to *Heikkilä et al.* [2011], a better ^{10}Be atmospheric mixing than previously assumed. The stratospheric ^{10}Be is transferred to the troposphere at mid-latitudes [e.g. *Bard and Frank,* 2006]. It seems reasonable to suppose that the atmospheric transport may have a negligible effect on ^{10}Be concentration in deep-sea sediments given that ^{10}Be residence time in the ocean is 500 to 1000 times higher.

^{10}Be content in marine sediments is also affected by oceanic reservoir effects (transport, adsorption and deposition processes) that depend on Be scavenging efficiency, residence time and particle composition affinities. Meaningless ^{10}Be concentrations have thus to be normalized and two proxies are currently used to retrieve the cosmogenic production signal: the ^{10}Be/^{230}Th$_{xs}$ ratio [e.g. *Frank et al*., 1997; *Christl et al.*, 2003, 2007, 2010; *Knudsen et al.,* 2008] and the authigenic ^{10}Be/^{9}Be ratio [*Bourlès et al.*, 1989; *Henken-Mellies et al.*, 1990; *Robinson et al.*, 1995; *Carcaillet et al*., 2003, 2004a, 2004b; *Leduc et al*., 2006]. Principles, as well as possible biases resulting from their use, were further summarized in *Ménabréaz et al.* [2011] and references therein. In their study, the authigenic ^{10}Be/^{9}Be methodology -confirmed for the first time by a ^{10}Be/^{230}Th$_{xs}$ cross-evaluation conducted on the same homogenized samples- has proven to reliably correct for ocean secondary contributions.

3.2 Beryllium isotopes sampling strategy determined from preliminary paleomagnetic results

A detailed paleomagnetic study will be presented in a future paper dedicated to a set of several cores collected in the same area. This paper limits itself to the relative paleointensity curve that has been the basis for Be sampling. Natural and artificial remanent magnetizations were measured on U-Channels using a 2G cryogenic magnetometer 760 SRM model coupled with an in-line Alternating Field (AF) demagnetizer. The Natural Remanent Magnetization (NRM) and Anhysteretic Remanent Magnetization (ARM) were measured after AF steps from 5 to 60 mT. After demagnetization at 30 mT, the NRM intensity /ARM intensity ratios were taken as the best proxy for the Relative PaleoIntensity (RPI) (Figure 2B). The major feature of this preliminary RPI record consists in a deep minimum located at 7.8 m expressing the occurrence of a geomagnetic dipole low (GDL).

The ^{10}Be sampling strategy was driven by the position of this GDL. The MD05-2920 sequence was sampled every 30 cm from 4.67 to 9.67 m, and every 10 cm between 6.27 and 8.67 m.

3.3 Sample preparation and Be isotopes extraction:

The 34 selected samples were dried and crushed in an agate mortar. Of the resulting homogenized powder, ~1g was leached using a 0.04M hydroxylamine (NH_2OH-HCl) in a 25% acetic acid leaching solution [*Bourlès et al.,* 1989]. This procedure avoid the leaching of detrital Be that would strongly bias the authigenic ^{10}Be/^{9}Be ratio through detrital ^{9}Be contamination.

The resulting leaching solution was then split into two aliquots: one 2ml aliquot was separated for natural ^{9}Be measurements using Flameless Atomic Adsorption Spectrophotometry, and the remaining solution was spiked using 300 µl of a 10^{-3} g/g ^{9}Becarrier solution (Sharlau®) before undergoing the chemical extraction procedure summarized below. Beryllium in the leachates was first chelated at pH 7 by acetylacetone. The obtained Be-acetylacetonates were then separated using an organic solvent extraction and decomposed in acid. Beryllium oxy-hydroxydes were finally precipitated at pH 8 before being oxidized to BeO at 800°C to perform AMS (Accelerator Mass Spectrometry) measurements [*Bourlès et al.,* 1989].

3.4 Measurements:

^{10}Be concentrations were measured using the new French AMS national facility "ASTER", operating at 5MV (CEREGE). ^{10}Be concentrations were calculated from the measured spiked ^{10}Be/^{9}Be ratios (see equation given by *Ménabréaz et al.* [2011]) normalized to the NIST 4325 international standard (^{10}Be/^{9}Be = 2.79×10^{-11} [*Nishiizumi et al.,* 2007]). Final ^{10}Be concentrations were all corrected for ^{10}Be radioactive decay using the half-life determined by *Chmeleff et al.* [2010] and *Korschinek et al.* [2010]. Uncertainties in the measured ^{10}Be/^{9}Be ratios and in the calculated ^{10}Be concentrations may result from counting statistics and instrumental error propagation [*Arnold et al.,* 2010], according to the standard propagation of uncertainties equation [e.g. *Taylor*, 1997]. Chemistry blank ratios range from 7.66 10^{-15} to 1.39 10^{-14} and are at least 1000 times lower than the sample ratios. Measured ratios and their uncertainties are presented in Table 1.

Natural ^{9}Be concentrations were measured using a graphite-furnace atomic absorption spectrophotometer equipped with a Zeeman effect background correction

(Thermo Scientific ICE 3400 installed at the CEREGE). The absorbance of each sample was repeatedly measured at incremental steps of standard addition. The analytical precision of final ^{9}Be concentrations was determined from the reproducibility of standard addition absorptions and the fit of standard addition lines, and ranges from 0.2% to 4.6% (see Table 1).

4. The authigenic ^{10}Be/^{9}Be record

Authigenic ^{10}Be concentrations vary from 9.56 x 10^{-15} g/g to 2.44 x 10^{-14} g/g and authigenic ^{9}Be concentrations vary from 1.79 x 10^{-7} g/g to 2.60 x 10^{-7} g/g, resulting in ^{10}Be/^{9}Be ratios that range from 4.57 x 10^{-8} to 1.20 x 10^{-7}. Sample concentration and ratio values are listed in Table 1. The ^{10}Be concentration profile shows a unique major enhancement reaching a peak at 767 cm which persists along the authigenic ^{10}Be/^{9}Be ratio profile (Figure 2A) in the form of ~1.7-fold increase of the ^{10}Be/^{9}Be ratio when compared to the average value calculated over the time interval spanned by this record (7.07 x 10^{-8}). This principal enhancement is recorded between ~737 cm and ~817 cm. The rest of the profile exhibits reduced variability, with slightly lower values before than after this major increase.

The RPI record, proxy of the geomagnetic dipole moment variation, and the authigenic ^{10}Be/^{9}Be ratio, proxy of the cosmogenic nuclide production, are inversely correlated (Figure 2). The main RPI low, located between ~850 cm and ~750 cm, and the main authigenic ^{10}Be/^{9}Be ratio enhancement, located between ~737 and ~817 cm, overlap to a large extent. The RPI minimum leads the authigenic $^{10}Be/^{9}Be$ ratio maximum by ~15 cm

Despite this slight delay which is coherent with the principle of the post-depositional magnetization lock-in depth, the two paleomagnetic and geochemical signatures must be interpreted as expressions of the same geomagnetic dipole low (GDL).

5. Age Model

The age model of core MD05-2920 is based on ten ^{14}C datings performed on the planktonic foraminifera *Globigerinoides ruber* (white), and on the correlation between the benthic $\delta^{18}O$ record and the reference benthic stack published by *Lisieki and Raymo* [2005] [Figure 3 in *Tachikawa et al.*, 2011]. After correction of the local reservoir age of 420 ± 60 yrs [*Mc Gregor et al.,* 2008], conventional ^{14}C ages were calibrated using the IntCal09 calibration set [*Reimer et al.*, 2009] and the Calib 6.1.0 software (http://intcal.qub.ac.uk/calib/)). The chronological reconstruction is presented in Figure 3C. Corresponding data can be found in Table 2. From these data, the sedimentation rates range between 12.3 and 16 cm/ka along the studied part of the MD05-2920 sequence.

6. Discussion

The authigenic $^{10}Be/^{9}Be$ record is plotted on its time scale in Figure 4a. The $^{10}Be/^{9}Be$ ratio peak can be seen recorded at ~40.8 ka, which allows its attribution to the Laschamp-related cosmogenic nuclide production enhancement in the atmosphere (see details on the chronology of the Laschamp event discussed by *Ménabréaz et al.* [2011]).

6.1 Comparison with the Laschamp ^{10}Be atmospheric overproduction records at mid and high latitudes.

The age of the authigenic $^{10}Be/^{9}Be$ maximum value at ~40.8 ka remarkably coincides (within uncertainties) with the age of the authigenic $^{10}Be/^{9}Be$ peak documenting the Laschamp-related GDL recorded at ~41 ka in Portuguese Margin sediment cores ([*Ménabréaz et al.*, 2011]; Figure 4b). Despite very different depositional settings, these authigenic $^{10}Be/^{9}Be$ records are in good overall correspondence over the whole studied time period. During the Laschamp GDL, the presented data indicate that the ^{10}Be production was enhanced by a factor of ~1.7 at that equatorial site (enhancement factors are determined from the average value over the time interval spanned by the records). This agrees, within respective uncertainties, with the ~1.9-fold increase measured in the authigenic $^{10}Be/^{9}Be$ ratio record of the Portuguese Margin [*Ménabréaz et al.*, 2011], and also with the ~1.7-fold increase previously reported by *Carcaillet et al.* [2004b] from a neighbouring core (Figure 4b). Such enhancement factors are also compatible with the near-doubling of the global (i.e. latitude integrated) ^{10}Be production during GDL, expected from the physically constrained algorithm [*Elsasser et al.*, 1956; *Lal*, 1988] and from numerical simulations [*Masarik and Beer*, 2009] describing the relation between geomagnetic moment and cosmogenic nuclides global production.

Furthermore, these sedimentary records of the ^{10}Be atmospheric overproduction linked to the Laschamp GDL are concomitant with the ^{10}Be-flux peak recorded in the

Greenland ice cap at Summit (Figure 4) [*Muscheler et al.*, 2005], dated at ~41 ka based on ice laminae counting (GICC05 timescale of the *NGRIP-dating group* [2006] and references therein]. This emphasises the simultaneity of the Laschamp ^{10}Be overproduction records in paleoclimatic archives at very different locations. Over the entire studied time interval, the presented authigenic ^{10}Be/^{9}Be records are remarkably similar both in time and in amplitude with the Greenland ^{10}Be-flux. This coherency of the signals observed for different archives located at different latitudes and in such various climatic and environmental conditions most likely allows ruling out the hypothesis that variability in ^{10}Be/^{9}Be ratios in core MD05-2920 arises primarily from changes in the continental runoff and oceanic regimes.

In addition to validating the pertinence of the authigenic ^{9}Be normalization to account for secondary effects, these observations more importantly demonstrate that the ^{10}Be production signal in marine sediments is a global signal because of the lack of any significant latitude effects. This remarkable correspondence also confirms that the Greenland ^{10}Be-flux signal over long time-scales is dominantly modulated by the geomagnetic dipole moment [e.g. *Muscheler et al.*, 2005], implying that a significant part of the ^{10}Be deposited in Greenland ice has been homogenized in the atmosphere. This supports a ^{10}Be residence time of several years in the atmosphere [*Baroni et al.*, 2011].

6.2 A marine stacked record of the ^{10}Be production rates.

The authigenic ^{10}Be/^{9}Be records obtained from sedimentary sequences from two different regions -West Equatorial Pacific (MD05-2920) and Northeast Atlantic (MD95-

2042 and MD04-2811 cores)- are normalized to their own average value and plotted on their own chronologies in Figure 5 (MD05-2920 chronological data are presented in Section 5 and Table 2; MD95-2042 and MD04-2811 chronological data are presented in *Ménabréaz et al.* [2011]).

These records are compared to the Greenland ^{10}Be flux (GRIP and GISP2 ice cores), normalized to its own average value and plotted in Figure 5 on its own chronology as established by multiparameter counting of annual layers [*Andersen et al.*, 2006; *NGRIP-dating group*, 2006; *Rasmussen et al.*, 2006]. The glacial part of this time scale has an estimated associated error of 2% back to 40 ka and of 5–10% back to 57 ka. The correspondence is remarkable despite noise and distortion introduced by 1) analytical uncertainties, 2) chronological uncertainties (e.g. linear interpolation between ~37 ka and 62 ka in the MD05-2920 core), and 3) recording processes (e.g. changes in sediment accumulation rate and/or sediment properties). A composite record of the normalized authigenic $^{10}Be/^{9}Be$ ratios is thus constructed and arithmetically averaged using a 1000-year sliding window offset by 500 years. Associated uncertainties (1σ) are standard deviations around computed average values.

The normalized authigenic $^{10}Be/^{9}Be$ stack (Figure 6; Table 3) indicates that the global 1000-year averaged ^{10}Be production rate increased by a factor of ~1.5 at ~41 ka (age of the Laschamp GDL) compared to the long-term average calculated over the 20-50 ka. No other significant enhancement of ^{10}Be production is evidenced over the studied time interval.

The comparison of the normalized authigenic $^{10}Be/^{9}Be$ stack with the Greenland ice sheet ^{10}Be-record (smoothed over a 1000-year window and plotted on its own timescale) evidences a remarkable similarity (Figure 6). This is especially noticeable considering that both records are obtained using very different techniques and recording archives. For the first time, the Greenland ^{10}Be deposition millennial-scale flux variations can be compared with an authigenic $^{10}Be/^{9}Be$ reference record composed by low and mid latitudes records. Their similarity confirms that the modulation mechanism is common and that they constitute proxies of the global atmospheric ^{10}Be production. Since there is no geomagnetic modulation of the cosmogenic nuclides production at high latitudes, the similarity of these ^{10}Be production records confirms that the major part of the ^{10}Be deposited in Greenland ice is transported from lower latitudes through atmospheric homogenization [e.g. *Muscheler et al.*, 2005; *Heikkilä et al.*, 2008]. The observed agreement of the Greenland ice record with oceanic sediment records located in high particle flux areas (where ^{10}Be residence time with respect to scavenging is ~500 yrs [*Anderson et al.*, 1990; *Ku et al.*, 1990]) also suggests that both signal attenuation and time lags potentially resulting from an oceanic ^{10}Be reservoir effect are minimized. Indeed, such settings reduce the ^{10}Be residence time in the water column and the effects of surface sediment mixing by the burrowing fauna.

6.3. Construction of a ^{10}Be-derived virtual dipole moment record

The normalized authigenic $^{10}Be/^{9}Be$ stack is then used to reconstruct the modulating dipole moment variation. Normalized $^{10}Be/^{9}Be$ values are calibrated using absolute VDM values determined from absolute paleointensities measured on lava flows and drawn from the literature. For coherency, the same absolute VDM values as in *Ménabréaz et al.* [2011] are taken from the GEOMAGIA-50 database, because they are assumed to be representative of the VDM values over the 20-50 ka time period. Since ^{10}Be production rates are inversely proportional to VDM values [*Elsasser et al.*, 1956; *Lal*, 1988], (1) the normalized $^{10}Be/^{9}Be$ maximum value (i.e. [1.52 ± 0.26] x 10^{-8}) was assigned to the minimum VDM value linked to the LE (i.e. 1.06 ± 0.05 x 10^{22} A.m^2 [*Levi et al*., 1990]), (2) the average of the normalized $^{10}Be/^{9}Be$ values lower than 0.78 (mean – 1 sigma) was assigned to the average of the VDM values higher than 8.70 A.m^2 (mean + 1 sigma), and (3) the average of the normalized $^{10}Be/^{9}Be$ values comprised between 0.78 and 1.12 ([mean ± 1 sigma] interval) was assigned to the average of the VDM values comprised between 3.62 and 8.70 A.m^2 ([mean ± 1 sigma] interval). This empirical polynomial fit obtained using the absolute VDM values is compared to the curve derived from Elsasser's algorithm, obtained using relative VDM values (as noted by *Lal*, [1992]) and applied to the normalized ^{10}Be production values derived from this study: their similarity reinforces the validity of the proposed calibration procedure (Figure 7). The polynomial fit between ^{10}Be and absolute VDM data is then applied to the whole ^{10}Be dataset. The ^{10}Be-derived absolute VDM reconstruction is shown in Figure 8 (data are listed in Table 3).

The ^{10}Be-derived absolute VDM reconstruction is compared to the reference relative paleointensity stacks, evidencing an overall good agreement with the GLOPIS-75 curve [*Laj et al.*, 2004], particularly between 36 and 51 ka (Figure 8). A major difference appears at 30-33 ka, where high RPI values in GLOPIS follow the reduction generally attributed to the Mono Lake excursion. The ^{10}Be-derived VDM record only shows a small amplitude reduction at ~34 ka followed by a progressive increase until ~22 ka, interrupted by another transient reduction at ~26 ka. The ^{10}Be-derived VDM record presents similar averaged values to the SINT 800 stack but points out a larger amplitude and narrower VDM reduction at the Laschamp age, due to the SINT-800 smoothing which results from stacking numerous records.

6.4 Geomagnetic implications

These cosmogenic nuclide production records and their translation as VDM records contribute to the understanding of the relation between the ^{10}Be production rates and the dipole moment values, and to the timing and quantification of the VDM reduction accompanying the geomagnetic excursions documented in the studied time interval. Indeed, the trends of the ^{10}Be-derived VDM stack result from the construction of robust chronologies along the two studied sedimentary sequences and are further supported by the tight correlation between the sedimentary and ice cores ^{10}Be production records. Estimates of durations and rates of changes are thus enabled.

While paleomagnetic sedimentary records rarely provide precise estimations of the duration of excursions due to 1) imperfect remanent magnetization acquisition in low intensity field, 2) remagnetization after recovery of higher intensity field [e.g. *Coe and Liddicoat,* 1994; *Roberts and Winklhofer,* 2004], and 3) latitudinal and longitudinal dependency of the geomagnetic vector variation, the ^{10}Be production records provide a global perspective on the timing and amplitude of the VDM variation.

The Laschamp Excursion

The global cosmogenic ^{10}Be enhancement at the time of the Laschamp excursion (~41 ka) recorded in the marine reference $^{10}Be/^{9}Be$ record is fully concordant with that reported from ^{10}Be deposition rates in the Greenland ice cores: when the dipole field vanishes (VDM ~$1x10^{22}$ $A.m^2$), the 1 ka average global ^{10}Be production rate is multiplied by ~1.5, while individual unsmoothed records report a 1.7- to 1.9- fold increase of the ^{10}Be production.

The duration of the enhancement phase can be estimated using, either the ^{10}Be value above "mean+1σ" which provides a maximum duration of 2500 years, or above "mean + 2σ", which provides a maximum duration of 1500 years. This provides the same estimated duration of VDM loss as that deduced from ice core records [*Wagner et al.*, 2000b; *Muscheler et al*., 2005] and from the GLOPIS-75 stack [*Laj et al.*, 2004].

The VDM collapse from ~11×10^{22} $A.m^2$ to ~1×10^{22} $A.m^2$ occurred between 48 and 41 ka, yielding an average pre-excursional VDM loss rate of ~ -1.4×10^{22} $A.m^2.ka^{-1}$. The main VDM loss occurred after 44 ka with a loss rate of ~ -1.5×10^{22} $A.m^2.ka^{-1}$. It is interesting to note that from archeomagnetic reconstructions [*Gallet et al.*, 2009], the computed VDM loss rate of ~ -2.7×10^{22} $A.m^2$ over the last millennium appears significantly higher than the Laschamp pre-excursional rates.

The Mono Lake Excursion

The ^{10}Be production reference records do not evidence any global significant increase in the atmospheric production of cosmogenic nuclides at the age of the Mono Lake excursion (~34 ka). The corresponding VDM value (4 x 10^{22} A.m^2) obtained from our reconstruction (Figure 8) is consistent with those determined from absolute paleointensities measured on lava flows (though it must be stressed that VDM values computed from low paleointensity data are, by definition, biased by non-dipole field contributions). In Hawaii, 9 of the 11 lavas recording the excursion yield VADM estimates of ~4 x 10^{22} A.m^2 [*Laj et al.*, 2002; *Teanby et al.*, 2002]. In the Canary Islands, the 3 studied lava flows yield VADM values of (4.3 ± 1.3), (1.6 ± 0.3), and (2.5 ± 0.8) × 10^{22} Am^2 [*Kissel et al.* 2011]. Compilation of New Zealand PI data [*Mochizuki et al*., 2006; *Cassidy and Hill* 2009] provides a VADM value of ~2.5 10^{22} A.m^2 [*Kissel et al.*, 2011].

The short duration of the GDL associated with the Mono Lake excursion may contribute to the lack of cosmogenic nuclide overproduction signature in marine archives. Taking into account a (standard) bioturbation depth of 15 cm, the related overproduction may not be recorded in these sequences. However, ^{10}Be ice records, despite their high resolution, do not exhibit either any overproduction signature either (see Muscheler et al., 2005), contrary to the ^{36}Cl record [*Wagner et al.*, 2000a]. The different response of these two cosmogenic nuclides, similarly produced through nuclear reactions induced in the atmosphere by cosmic ray particles has led to questions concerning the reliability of the ^{36}Cl peak [see *Delmas et al.*, 2004].

7. Conclusion and perspectives

The $^{10}Be/^{9}Be$ record of the MD05-2920 sediment core is the first reliable authigenic $^{10}Be/^{9}Be$ evidence of cosmogenic nuclide ^{10}Be overproduction at low latitude at the age of the Laschamp excursion (41 ka). Together with other records of marine and terrestrial archives it confirms the global synchronicity of the ^{10}Be overproduction in the atmosphere generated by the loss of the geomagnetic dipole. The compilation of authigenic $^{10}Be/^{9}Be$ marine records indicates that the global ^{10}Be production rates at 41 ka were enhanced by a ~1.5 factor compared to the average over the 20-60 ka interval. The comparison of the authigenic $^{10}Be/^{9}Be$ marine stack with the Greenland ^{10}Be flux record (smoothed by 1000-year averaging) evidences a good coherency of the timing and amplitude of ^{10}Be production at high, mid and low latitudes. This confirms that the ^{10}Be overproduction signal has a global significance, as expected from a geomagnetic dipole moment loss.

The calibration of the sedimentary $^{10}Be/^{9}Be$ stack using absolute virtual dipole moment values provides an independent tool to reconstruct geomagnetic dipole moment variations. This allows computing the loss rate leading to the Laschamp dipole minimum (~ -1.5×10^{22} $A.m^{2}.ka^{-1}$). This constitutes an interesting criterion to assess the loss rate of the historical field.

In constrast with the relavant signatures in the GLOPIS-75 relative paleointensity stack and in absolute paleointensity data sets, the absence of significant cosmogenic response at 34 ka suggests that the Mono Lake dipole low was hardly sufficient to trigger a significant cosmogenic overproduction. This demonstrates that if the Mono lake excursion really occurred at that time, the duration and amplitude of the dipole weakening were very limited compared to that of the Laschamp.

The ^{10}Be overproduction quantified in this study constitutes a reliable basis to calibrate radiocarbon production and *in situ* cosmogenic nuclides production. For example, it can help to understand the atmospheric ^{14}C concentration variations recorded near 41 ka and near 34 ka in delta ^{14}C series [e.g. *Hughen et al.,* 2004; *Reimer et al.*, 2009], which were probably produced by the Laschamp and Mono Lake geomagnetic dipole lows.

The ^{10}Be production peak linked to the Laschamp dipole low can be used as a global tie point for correlation of high-resolution paleoclimatic series obtained from high quality archives.

Acknowledgements:

This work is a contribution to the MAG-ORB (ANR- 09-BLAN-0053-01) project, which is funded by the French Agence Nationale de la Recherche (ANR). We aknowledge V. Guillou for technical assistance during chemical procedures, and F. Demory for help in U-channel sampling and during paleomagnetic data acquisition. R. Muscheler kindly provided the ^{10}Be ice cores data used in this study. We also thank here M. Arnold, G. Aumaître, and K. Keddadouche for their valuable assistance during ^{10}Be measurements at the ASTER AMS national facility (CEREGE, Aix-en-Provence), which is supported by the INSU/CNRS, the French Ministry of Research and Higher Education, IRD and CEA. We acknowledge the scientific and technical crew of R.V. *Marion Dufresne* who collected core MD05-2920 during the MD148-PECTEN Cruise. We thank Prof. M. Frank and an anonymous reviewer for their helpful comments in preparing the final version of the manuscript.

Reference list:

Andersen, K.K., Svensson, A., Rasmussen, S.O., Steffensen, J.P., Johnsen, S.J., Bigler, M., Röthlisberger, R., Ruth, U., Siggaard-Andersen, M.-L., Dahl-Jensen, D., Vinther, B.M., Clausen, H.B., 2006. The Greenland Ice Core Chronology 2005, 15–42 ka. Part 1: constructing the time scale. Quat. Sci. Rev. 25, 246–257.

Anderson R.F., Y. Lao, W.S. Broecker, S.E Trumbore., H.J. Hofmann, and W. Wolfli (1990), Boundary scavenging in the Pacific Ocean: a comparison of ^{10}Be and ^{231}Pa, *Earth and Planet. Sci. Lett. 96*, 287-304.

Arnold, M., S. Merchel, D.L. Bourlès, R. Braucher, L. Benedetti, R.C. Finkel, G. Aumaître, A. Gottdang, and M. Klein (2010), The French accelerator mass spectrometry facility ASTER: Improved performance and developments, *Nucl. Instrum. Methods Phys. Res. Sect. B 268*, 1954-1959.

Bard, E., and M. Frank, (2006), Climate change and solar variability: What's new under the sun? *Earth and Planet. Sci. Lett. 248*, 1–14.

Baroni, M., E. Bard, J.R Petit, O. Magnan, and D.L Bourlès (2011), Volcanic and solar activity, and atmospheric circulation influences on cosmogenic 10Be fallout at Vostok and Concordia (Antarctica) over the last 60 years., *Geochim. Cosmochim. Acta*, *ISSN 0016-7037*, doi: 10.1016/j.gca.2011.09.002.

Beaufort, L., A.W. Droxler, M.-T Chen, and party, t.m.o.t.s., 2005. MD148 / IMAGES XIII, PECTEN 2005 Cruise Report.

Beer, J., A. Blinov, G. Bonani, R.C. Finkel, H.J. Hofman, B. Lelmann, H. Oeschger, A. Sigg, J. Schwander, T. Staffelbach, B. Stauffer, M. Suter, and W. Wolfli, (1990), Use of ^{10}Be in polar ice to trace the 11-year cycle of solar activity, *Nature 347*, 164-166.

Benson, L., J. Liddicoat, J. Smoot, A Sarna-Wojcicki. R. Negrini, and S. Lund, (2003), Age of the Mono Lake excursion and associated tephra, *Quat. Sci. Rev. 22*, 135-140.

Bonhommet, N., and J. Babkine (1967), Sur la présence d'aimantations inverses dans la Chaîne des Puys — Massif Central, France, *C.R.A.S. Paris 264*, 92.

Bonhommet, N., and J. Zahringer (1969), Paleomagnetism and potassium argon age determinations of the Laschamp geomagnetic polarity event, *Earth Planet. Sci. Lett. 6*, 43–46.

Bourlès, D., G.M. Raisbeck, and F. Yiou (1989), ^{10}Be and ^{9}Be in marine sediments and their potential for dating, *Geochim. Cosmochim. Acta 53*, 443-452.

Carcaillet, J., N. Thouveny, and D.L. Bourlès (2003), Geomagnetic moment instability between 0.6 and 1.3 Ma from cosmonuclide evidence, *Geophys. Res. Lett. 30*, 1792.

Carcaillet, J., D.L. Bourlès, and N. Thouveny (2004a), Geomagnetic dipole moment and 10Be production rate intercalibration from authigenic $^{10}Be/^{9}Be$ for the last 1.3 Ma, *Geochem. Geophys. Geosyst. 5*, 397-412, Q05006, doi: 10.1029/2003GC000641.

Carcaillet, J., D.L. Bourlès, N. Thouveny, and M. Arnold, (2004b), A high resolution authigenic $^{10}Be/^{9}Be$ record of geomagnetic moment variations over the last 300 ka from sedimentary cores of the Portuguese margin, *Earth Planet. Sci. Lett. 219*, 397-412.

Cassata, W.S., B.S. Singer, and J. Cassidy, (2008), Laschamp and Mono Lake geomagnetic excursions recorded in New Zealand, *Earth Planet. Sci. Lett. 268*, 76-88.

Cassidy, J., and M. J. Hill (2009), Absolute palaeointensity study of the Mono Lake excursion recorded by New Zealand basalts, *Phys. Earth Planet. Inter. 172*, 225–234.

Channell, J. (2006), Late Brunhes polarity excursions (Mono Lake, Laschamp, Iceland Basin and Pringle Falls) recorded at ODP Site 919 (Irminger Basin), *Earth Planet. Sci. Lett. 244*, 378-393.

Channell, J.E.T., C. Xuan, and D.A. Hodell, (2009), Stacking paleointensity and oxygen isotope data for the last 1.5 Myr (PISO-1500), *Earth Planet. Sci. Lett. 283*, 14-23.

Chauvin A., R.A. Duncan, N. Bonhommet, and S. Levi (1989), Paleointensity of the earth's magnetic field and K–Ar dating of the Louchadière volcanic flow (central France): New evidence for the Laschamp Excursion, *Geophys. Res. Lett. 16*, 1189–1192.

Chmeleff, J., F. von Blanckenburg, K. Kossert, and D. Jakob (2010), Determination of the ^{10}Be half-life by multicollector ICP-MS and liquid scintillation counting, *Nucl. Instrum. Methods Phys. Res. Sect. B 268*, 192-199.

Christl, M., C. Strobl, and A. Mangini, (2003), Beryllium-10 in deep-sea sediments: a tracer for the Earth's magnetic field intensity during the last 200,000 years, *Quat. Sci. Rev. 22*, 725-739.

Christl, M., A. Mangini, and P.W. Kubik (2007), Highly resolved Beryllium-10 record from ODP Site 1089--A global signal? *Earth Planet. Sci. Lett. 257*, 245-258.

Christl, M., J. Lippold, F. Steinhilber, F. Bernsdorff, and A. Mangini, (2010), Reconstruction of global ^{10}Be production over the past 250 ka from highly accumulating Atlantic drift sediments, *Quat. Sci. Rev. 29*, 2663-2672.

Coe, R.S., and J.C. Liddicoat (1994), Overprinting of natural magnetic remanence in lake sediments by subsequent high intensity field, *Nature 367*, 57-59.

Condomines M. (1980), Age of the Olby-Laschamp geomagnetic polarity event, *Nature 286*, 697–699.

Cresswell, G.R. (2000), Coastal currents of northern Papua New Guinea, and the Sepik River Outflow, *Mar. Freshw. Res. 51*, 553-564.

Denham, C.R., and A. Cox, (1971), Evidence that the Laschamp polarity event did not occur 13300–30400 years ago, *Earth Planet. Sci. Lett. 13*, 181-190.

Delmas R.J., J. Beer, H.A. Synal, R. Muscheler, J.R. Petit, and M. Pourchet (2004), Bomb-test ^{36}Cl measurements in Vostok snow (Antartica) and the use of ^{36}Cl as a dating tool for deep ice cores, *Tellus 56B*, 492-498.

Elsasser, W., E.P. Ney, and J.R. Winckler (1956), Cosmic-ray intensity and geomagnetism, *Nature 178*, 1226-1227.

Finkel, R.C., and K. Nishiizumi (1997), Beryllium-10 concentrations in the Greenland Ice Sheet Project 2 ice core from 3–40 ka, *J. Geophys. Res. 102*, 26699-26706.

Frank, M., B. Schwarz, S. Baumann, P.W. Kubik, M. Suter, and A. Mangini (1997), A 200 kyr record of cosmogenic radionuclide production rate and geomagnetic field intensity from ^{10}Be in globally stacked deep-sea sédiments, *Earth Planet. Sci. Lett. 149*, 121-129.

Frank, M. (2000), Comparison of cosmogenic radionuclide production and geomagnetic field intensity over the last 200,000 years, *Phil. Trans. R. Soc. Lond. A 358*, 1089-1107.

Gallet Y., A. Genevey, M. Le Goff, N. Warmé, J. Gran-Aymerich, and A. Lefèvre (2009), On the use of archeology in geomagnetism and vice-versa : Recent developments in archeomagnetism, *C.R Phys. 10*, 630-648.

Gillot, P.Y., J. Labeyrie, C. Laj, G. Valladas, G. Guerin, G. Poupeau, and G. Delibrias (1979), Age of the Laschamp geomagnetic polarity excursion revisited, *Earth Planet. Sci. Lett. 42*, 444–450.

Guillou, H., B.S. Singer, C. Laj, C. Kissel, S. Scaillet, and B.R. Jicha (2004), On the age of the Laschamp geomagnetic excursion, *Earth Planet. Sci. Lett. 227*, 331-343.

Guyodo, Y., and J.P. Valet (1999), Global changes in intensity of the Earth's magnetic field during the past 800 kyr, *Nature 399*, 249-252.

Hall, C.M., and D. York (1978), K–Ar and ^{40}Ar/^{39}Ar age of the Laschamp geomagnetic polarity reversal, *Nature 274*, 462–464.

Hanna, R. L., and K. L. Verosub (1989), A review of lacustrine paleomagnetic records from Western North America : 0-40000 years BP, *Phys. Earth Planet. Inter. 56*, 76-95.

Heikkilä, U., J. Beer, and J. Feichter (2008), Meridional transport and deposition of atmospheric ^{10}Be, *Atmos. Chem. Phys. Discuss.*, *8*, 16819–16849, 2008 www.atmos-chem-phys-discuss.net/8/16819/2008/

Heikkilä, U., J. Beer, J.A. Abreu, and F. Steinhilber (2011), On the Atmospheric Transport and Deposition of the Cosmogenic Radionuclides (^{10}Be): A Review, *Space Sci. Rev.*, doi: 10.1007/s11214-011-9838-0.

Henken-Mellies, W.U., J. Beer, F. Heller, K.J. Hsü¸ C. Shen, G. Bonani, H.J. Hofmann, M. Suter, and W. Wölfli (1990), ^{10}Be and ^{9}Be in South Atlantic DSDP Site 519: Relation to geomagnetic reversals and to sediment composition, *Earth Planet. Sci. Lett. 98*, 267-276.

Hughen, K., S. Lehman, J. Southon, J. Overpeck, O. Marchal, C. Herring, and J. Turnbull (2004), ^{14}C Activity and Global Carbon Cycle Changes over the Past 50,000 Years, *Science 303*, 202-207.

Kawahata, H., A. Suzuki, and H. Ohta (2000), Export fluxes in the Western Pacific Warm Pool, *Deep-Sea Res.I 47*, 2061-2091.

Kent, D.V., S.R. Hemming, and B.D. Turrin (2002), Laschamp Excursion at Mono Lake? *Earth Planet. Sci. Lett. 197*, 151-164.

Kineke, G.C., K.J. Woolfe, S.A. Kuehl, J.D. Milliman, T.M. Dellapenna, and R.G. Purdon (2000), Sediment export from the Sepik River, Papua New Guinea: evidence for a divergent sediment plume, *Cont. Shelf Res. 20*, 2239-2266.

Kissel, C., H. Guillou, C. Laj, J.C. Carracedo, S. Nomade, F. Perez-Torrado, and C. Wandres (2011), The Mono Lake excursion recorded in phonolitic lavas from Tenerife (Canary Islands): paleomagnetic analyses and coupled K/Ar and Ar/Ar dating, *Phys. Earth Planet. Inter. 187*, 232-244.

Knudsen, M.F., G.M. Henderson, M. Frank, C. Mac Niocaill, and P.W. Kubik (2008), In-phase anomalies in Beryllium-10 production and palaeomagnetic field behaviour during the Iceland Basin geomagnetic excursion, *Earth Planet. Sci. Lett. 265*, 588-599.

Korhonen, K., F. Donadini, P. Riisager, and L.Pesonen (2008), GEOMAGIA50: an archeointensity database with PHP and MySQL, *Geochem. Geophys. Geosyst. 9 (4)*, Q04029, doi: 10.1029/2007GC001893.

Korschinek, G., A. Bergmaier, T. Faestermann, U.C. Gerstmann, K. Knie, G. Rugel, A. Wallner, I. Dillmann, G. Dollinger, C.L. von Gostomski, K. Kossert, M. Maiti, M. Poutivtsev, and A. Remmert (2010), A new value for the half-life of ^{10}Be by Heavy-Ion Elastic Recoil Detection and liquid scintillation counting, *Nucl. Instr. Meth. in Phys. Res. Sect. B 268*, 187-191.

Kristjansson, L., and A.A. Gudmundsson, (1980), Geomagnetic excursions in late-glacial basalt outcrop in south-western Iceland, *Geophys. Res. Lett. 7*, 337–340.

Ku, T.L., M. Kusakabe, C.I. Measures, J.R., Southon, G. Cusimano, J.S. Vogel, D.E. Nelson, and S. Nakaya (1990), Beryllium isotope distribution in the western North Atlantic : a comparison to the Pacific, *Deep-Sea Res. 37*, 795-808.

Laj, C., C. Kissel, A. Mazaud, J.E.T. Channell, and J. Beer (2000), North Atlantic paleointensity stack since 75 ka (NAPIS-75) and the duration of the Laschamp event, *Philos. Trans. R. Soc. Lond. 358*, 1009–1025.

Laj, C., C. Kissel, V. Scao, J. Beer, D.M. Thomas, H. Guillou, R. Muscheler, and G. Wagner (2002), Geomagnetic intensity and inclination variations at Hawaii for the past 98 kyr from core SOH-4 (Big Island): a new study and a comparison with existing contemporary data, *Phys. Earth Planet. Inter. 129*, 205–243.

Laj, C., C. Kissel, and J. Beer (2004), High resolution global paleointensity stack since 75 kyr (GLOPIS-75) calibrated to absolute values, In: Channell, J.E.T., D.V. Kent, W. Lowrie, and J.G. Meert, (Eds.), Timescales of the Paleomagnetic Field, *Geophys. Monogr. 145*.

Lal, D. (1988), Theoretically expected variations in the terrestrial cosmic-ray production rates of isotopes, *Soc. Italia. di Fisica-Bologna-Italy XCV corso*, 216-233.

Lal, D. (1992), Expected secular variations in the global terrestrial production rate of radiocarbon, In: Bard, E., and W.S. Broecker (Eds.), The Last Deglaciation: Absolute and Radiocarbon Chronologies, Series I, *Global Environmental Change 2*, 114–126.

Lal, D., and B. Peters (1967), Cosmic ray produced radioactivity on the Earth, in: Flugge, S. (Ed.), *Handb. Phys. Springer*, pp. 551-612.

Leduc, G., N. Thouveny, D.L Bourlès, C.L. Blanchet, and J.T Carcaillet (2006), Authigenic ^{10}Be/^{9}Be signature of the Laschamp excursion: A tool for global synchronisation of paleoclimatic archives, *Earth Planet. Sci. Lett. 245*, 19-28.

Levi, S., H. Gudmunsson, R.A. Duncan, L. Kristjansson, P.V Gillot, and S.P. Jacobsson (1990), Late Pleistocene geomagnetic excursion in Icelandic lavas: Confirmation of the Laschamp excursion, *Earth Planet. Sci. Lett. 96*, 443–457.

Liddicoat, J.C. (1992), Mono Lake Excursion in Mono Basin, California, and at Carson Sink and Pyramid Lake, Nevada, *Geophys. J. Intern. 108*, 442-452.

Lisiecki, L.E. and M.E. Raymo (2005), A Pliocene-Pleistocene stack of 57 globally distributed benthic δ^{18}O record, *Paleoceanography*, *20*, 1-17, doi:10.1029/2004PA001071

Lund, S.P., M. Schwartz, L. Keigwin, and T. Johnson (2005), Deep-sea sediment records of the Laschamp geomagnetic field excursion (<41,000 calendar years before present), *J. Geophys. Res. 110*, Q12006.

Lund, S.P., J.S. Stoner, J.E.T. Channell, and G. Acton (2006), A summary of Brunhes paleomagnetic field variability recorded in ODP Cores, *Phys. Earth Planet. Int. 156*, 194–204.

Masarik, J., and J. Beer (1999), Simulation of particle fluxes and cosmogenic nuclide production in the Earth's atmosphere, *J. Geophys. Res. 104*, 12099-12111.

Masarik, J., and J. Beer (2009), An updated simulation of particle fluxes and cosmogenic nuclide production in the Earth’s atmosphere. *J. Geophys. Res. 114*, D1110, doi:10.1029/2008JD010557.

McGregor, H.V., M.K. Gagan, M.T. McCulloch, E. Hodge, and G. Mortimer (2008), Mid-Holocene variability in the marine ^{14}C reservoir age for northern coastal Papua New Guinea, *Quat. Geochronol. 3*, 213-225.

Ménabréaz, L., N. Thouveny, D. L Bourlès, P. Deschamps, B. Hamelin, and F. Demory (2011), The Laschamp geomagnetic dipole low expressed as a cosmogenic ^{10}Be atmospheric overproduction at ~41 ka, *Earth Planet. Sci. Lett. 312*, 305-317.

Milliman, J.D., K.L. Farnsworth, and C.S. Albertin (1999), Flux and fate of fluvial sediments leaving large islands in the East Indies, *J. Sea Res. 41*, 97-107.

Mochizuki, N., H. Tsunakawa, H. Shibuya, T. Tagami, A. Ozawa, J. Cassidy, and I.E.M. Smith (2004), K–Ar ages of the Auckland geomagnetic excursions, *Earth Planets Space 56*, 283–288.

Mochizuki, N., H.Tsunakawa, H. Shibuya, J. Cassidy, and I.E.M. Smith (2006), Paleointensities of the Auckland geomagnetic excursions, *Phys. Earth Planet. Inter. 154*, 168–179.

Mochizuki, N., H.Tsunakawa, H. Shibuya, T. Tagami, A. Ozawa, and I.E.M. Smith (2007), Further K–Ar dating and paleomagnetic study of the Auckland geomagnetic excursions, *Earth Planets Space 59*, 755–761.

Muscheler, R., J. Beer, P.W. Kubik, and H.A. Synal (2005), Geomagnetic field intensity during the last 60,000 years based on ^{10}Be and ^{36}Cl from the Summit ice cores and ^{14}C. *Quat. Sci. Rev. 24,* 1849-1860.

Negrini, R.M., J.O Davis, and K.L. Verosub (1984), Mono Lake geomagnetic excursion found at Summer Lake, Oregon, *Geology 12*, 643-646.

Negrini, R., K.F Erbes, A.M. Herrera, A.P Roberts, A. Cohen, M. Palacios-Fest, P.E. Wigand, and F. Foit (2000), A paleoclimate record for the past 250,000 years from Summer Lake, Oregon, USA: I. Age control and magnetic lake level proxies, *J. Paleolimn. 24*, 125-149.

Nishiizumi, K., M. Imamura, M.W. Caffee, J.R. Southon, R.C. Finkel, and J. McAninch (2007), Absolute calibration of 10Be AMS standards, *Nucl. Instr. Meth. in Phys. Res. Sect. B 258*, 403-413.

NGRIP-dating-group (2006), Greenland Ice Core Chronology 2005 (GICC05), IGBP PAGES/World Data Center for Paleoclimatology Data Contribution Series # 2006-118. NOAA/NCDC Paleoclimatology Program, Boulder CO, USA.

Nowaczyk, N.R., and J. Knies (2000), Magnetostratigraphic results from the eastern Arctic ocean: AMS ^{14}C ages and relative paleointensity data of the mono lake and Laschamp geomagnetic reversal excursions, *Geophys. J. Intern. 140*, 185-197.

Plenier, G., J.P. Valet, G. Guérin, J.C Lefêvre, M. LeGoff, and B. Carter-Stiglitz (2007), Origin and age of the directions recorded during the Laschamp event in the Chaîne des Puys (France), *Earth Planet. Sci. Lett. 259*, 414-431.

Raisbeck, G.M., F. Yiou, M. Fruneau, J.M Loiseaux, M. Lieuvin, and J.C. Ravel (1981), Cosmogenic Be-10/Be-7 as a probe of atmospheric transport processes, G*eophys. Res. Lett. 8*, 1015-1018.

Raisbeck, G. M., F. Yiou, J. Jouzel, J.R Petit, E. Bard, and N. I Barkov (1992), ^{10}Be deposition at Vostok, Antarctica, during the last 50000 years and its relationship to possible cosmogenic production variations during this period, in: Bard, E., and W.S. Broecker (Eds.), The Last Deglaciation: Absolute and Radiocarbon Chronologies, Series I, *Global Environmental Change 2*, 127–139.

Rasmussen, S.O., Seierstad, I.K., Andersen, K.K., Bigler, M., Dahl-Jensen, D., Johnsen, S.J., 2006. NGRIP, GRIP, and GISP2 Synchronization Match Points. IGBP PAGES/World Data Center for Paleoclimatology. Data Contribution Series # 2006-120. NOAA/NCDC Paleoclimatology Program, Boulder CO, USA.

Reimer, P.J., M.G.L. Baillie, E. Bard, A. Bayliss, J.W Beck, P.G. Blackwell, C. Bronk Ramsey, C.E. Buck, G.S. Burr, R.L. Edwards, M. Friedrich, P.M. Grootes, T.P Guilderson, I. Hajdas, T.J. Heaton, A.G Hogg, K.A. Hughen, K.F. Kaiser, B. Kromer, G. McCormac, S. Manning, R.W Reimer, D.A. Richards, J.R. Southon, S. Talamo, C.S.M. Turney, J. van der Plicht, and C.E Weyhenmeyer (2009), IntCal09 and Marine09 radiocarbon age calibration curves, 0-50000 Years cal BP, *Radiocarbon 51*, 1111-1150.

Roberts, A.P., and M. Winklhoferb (2004), Why are geomagnetic excursions not always recorded in sediments? Constraints from post-depositional remanent magnetization lock-in modelling, *Earth Planet. Sci. Lett. 227*, 345-359.

Robinson, C., G.M Raisbeck, F. Yiou, B. Lehman, and C. Laj (1995), The relationship between ^{10}Be and geomagnetic field strength records in central North Atlantic sediments during the last 80 ka, *Earth Planet. Sci. Lett. 136*, 551-557.

Roperch, P., N. Bonhommet, and S. Levi (1988), Paleointensity of the earth's magnetic field during the Laschamp excursion and its geomagnetic implications, *Earth Planet. Sci. Lett. 8*8, 209–219.

Shibuya, H., J. Cassidy, I.E.M. Smith, and T. Itaya (1992), A geomagnetic excursion in the Brunhes epoch recorded in New Zealand basalts, *Earth Planet. Sci. Lett. 111*, 41–48.

Singer, B.S., H. Guillou, B.R Jicha, C. Laj, C. Kissel, B.L Beard, and C.M. Johnson (2009), ^{40}Ar/^{39}Ar, K-Ar and ^{230}Th-^{238}U dating of the Laschamp Excursion: A radioisotopic tie-point for ice core and climate chronologies, *Earth Planet. Sci. Lett. 286,* 80-88.

Tachikawa, K., O. Cartapanis, L. Vidal, L. Beaufort, T. Barlyaeva, and E. Bard (2011), The precession phase of hydrological variability in the Western Pacific Warm Pool during the past 400 ka, *Quat. Sc. Rev. 30*, 3716-3727

Taylor, J.R. (1997), An Introduction to Error Analysis. The study of Uncertainties in Physical Measurements, *Second ed., University Science Books, Sausalito, USA*.

Teanby, N., C. Laj, D. Gubbins, and M. Pringle (2002), A detailed palaeointensity and Inclination record from drill core SOH1 on Hawaii, *Physics Earth Planet. Inter. 131*, 101-140.

Thouveny, N., and K.M. Creer (1992), On the brievity of the Laschamp Excursion, *Bull. Soc. Géol. Fr. 6*, 771–780.

Thouveny, N., J. Carcaillet, E. Moreno, G. Leduc, and D. Nérini (2004), Geomagnetic moment variation and paleomagnetic excursions since 400 kyr BP: a stacked record from sedimentary sequences of the Portuguese margin, *Earth Planet. Sci. Lett. 219*, 377-396.

Vlag, P., N. Thouveny, D. Williamson, P. Rochette, and F. Ben-Atig (1996), Evidence for a geomagnetic excursion recorded in the sediments of Lac St. Front, France: a link with the Laschamp Excursion? *J. Geophys. Res. 101*, 28211–28230.

Wagner, G., J. Beer, C., Laj, C. Kissel, J. Masarik, R. Muscheler, and H.A. Synal (2000a), Chlorine-36 evidence for the Mono Lake event in the Summit GRIP ice core, *Earth Planet. Sci. Lett. 181*, 1-6.

Wagner, G., J. Masarik, J. Beer, S. Baumgartner, D. Imboden, P.W Kubik, H.A Synal, and M. Suter (2000b), Reconstruction of the geomagnetic field between 20 and 60 kyr BP from cosmogenic radionuclides in the GRIP ice core, *Nucl. Instrum. Methods Phys. Res. Sect. B 172*, 597-604.

Wang, B., S.C. Clemens, and P. Liu (2003), Contrasting the Indian and East Asian monsoons: implications on geologic timescales, *Mar. Geol. 201*: 5-21.

Wang, Y.J., H. Cheng, R.L. Edwards, Z.S An, J.Y. Wu, C.C. Shen, and J.A. Dorale (2001), A High-Resolution Absolute-Dated Late Pleistocene Monsoon Record from Hulu Cave, China, *Science 294*, 2345-2348.

Webster, P.J., V.O Magana, T.N. Palmer, J. Shukla, R.A. Tomas, M. Yanai, and T. Yasunari (1998), Monsoon: Processes, predictability, and prospects for prediction, *J. Geophys. Res. 103(C7)*, 14451-14,10.

Yiou, F., G.M. Raisbeck, S. Baumgartner, J. Beer, C. Hammer, S. Johnsen, J. Jouzel, P.W. Kubik, J. Lestringuez, M. Stiévenard, M. Sutter, and P. Yiou (1997), Beryllium 10 in the Greenland Ice Core Project ice core at Summit, Greenland, *J. Geophys. Res. 102*, 26783-26794.

Zic, M., R. Negrini, and P.E. Wigand (2002), Evidence of synchronous climate change across the Northern Hemisphere between the North Atlantic and the northwestern Great Basin, United States, *Geology 30*, 635–638.

Zimmerman, S.H., S.R. Hemming, D.V. Kent, and S.Y. Searle (2006), Revised chronology for late Pleistocene Mono Lake sediments based on paleointensity correlation to the global reference curve, *Earth Planet. Sci. Lett. 252*, 94-106.

Figure Captions :

Figure 1. A. Location map of the MD05-2920 coring site in the Bismarck Sea, on the Papua New Guinea northern margin. B. Location of the marine sediment cores used in this study: MD05-2020 core located North of Papua New Guinea (NPNG), MD04-2811 and MD95-2042 cores located on the Portuguese Margin. Location of the GRIP and GISP2 ice cores at Summit (Greenland).

Figure 2. A. The $^{10}Be/^{9}Be$ record along core MD05-2920. B. The NRM and ARM intensities are both demagnetized at 30mT AF step along core MD05-2920 and provide a ratio considered as the best Relative Paleointensity proxy. C. $\delta^{18}O$ measured on benthic foraminifer *Uvigerina peregrina* (Tachikawa et al., 2011). D. Chronostratigraphic markers in MD05-2920 sediments, and the depth-age relationship. Green dots are radiocarbon dated levels, and the blue dot is the MIS-3 MIS-4 transition tie point. Between these points, the age model is based on linear interpolation.

Figure 3. (a) ^{10}Be deposition flux (10^6 atoms/cm^2/yr) record at Summit (Greenland) in GIPS2 and GRIP ice cores [*Finkel et al.*, 1997; *Yiou et al*., 1997; *Muscheler et al.*, 2005]. Authigenic $^{10}Be/^{9}Be$ ratios (10^{-8}) records in the Portuguese Margin (b) and Papua New Guinea (c) sediments.

Figure 4. Records of ^{10}Be atmospheric production variations between 20 and 60 ka. Dots correspond to the authigenic $^{10}Be/^{9}Be$ ratios from MD04-2811 (blue dots), MD05-2920 (red dots) and MD95-2042 (black dots). In grey, the Greenland ^{10}Be deposition flux variations. All data series are normalized to their own mean values, and plotted on their own chronological scales.

Figure 5. Variations of the ^{10}Be production in the atmosphere during the 20-50 ka period. In red, the authigenic ^{10}Be/^{9}Be composite record, and the associated 1σ uncertainties. It is compared with the Greenland ^{10}Be-Flux record (In grey), and its 1000-year smoothed version (black curve). The Greenland record is normalized to its own mean value, and plotted on its own chronological scale (see text).

Figure 6. Calibration of the normalized ^{10}Be/^{9}Be (proxy of the normalized ^{10}Be production) values using Virtual Dipole Moments (VDM) values provided by the GEOMAGIA-50 database [*Korhonen et al*., 2008], and the polynomial fit used to derive Virtual Dipole Moments (VDM): $y = 32.973 - 42.156x + 13.921x^2$. The normalized ^{10}Be/^{9}Be intermediate and minimum clusters are calculated using values comprised within the « mean ± 1σ » range, and using values less than « mean - 1σ », respectively. Associated error bars correspond to the standard deviation of the values used for averaging. Grey dots indicate normalized dipole moments obtained after application of Elsasser's algorithm [see *Lal*, 1992] on the normalized ^{10}Be/^{9}Be data.

Figure 7. ^{10}Be-based VDM reconstruction (in 10^{22} Am^2) and associated 1-sigma uncertainties, compared to paleomagnetic VADM reconstructions (GLOPIS-75 and SINT 800 reference records) over the 20- 50 ka interval. The grey band represents the GLOPIS-75 1 sigma envelop [*Laj et al.*, 2004] plotted on the GICC05 time-scale, and the black curve is the SINT 800 reconstruction [*Guyodo and Valet*, 1999]. Each data series is plotted on its own time scale. The dotted line shows the present-day VADM value of ~8 x 10^{22} A.m^2.

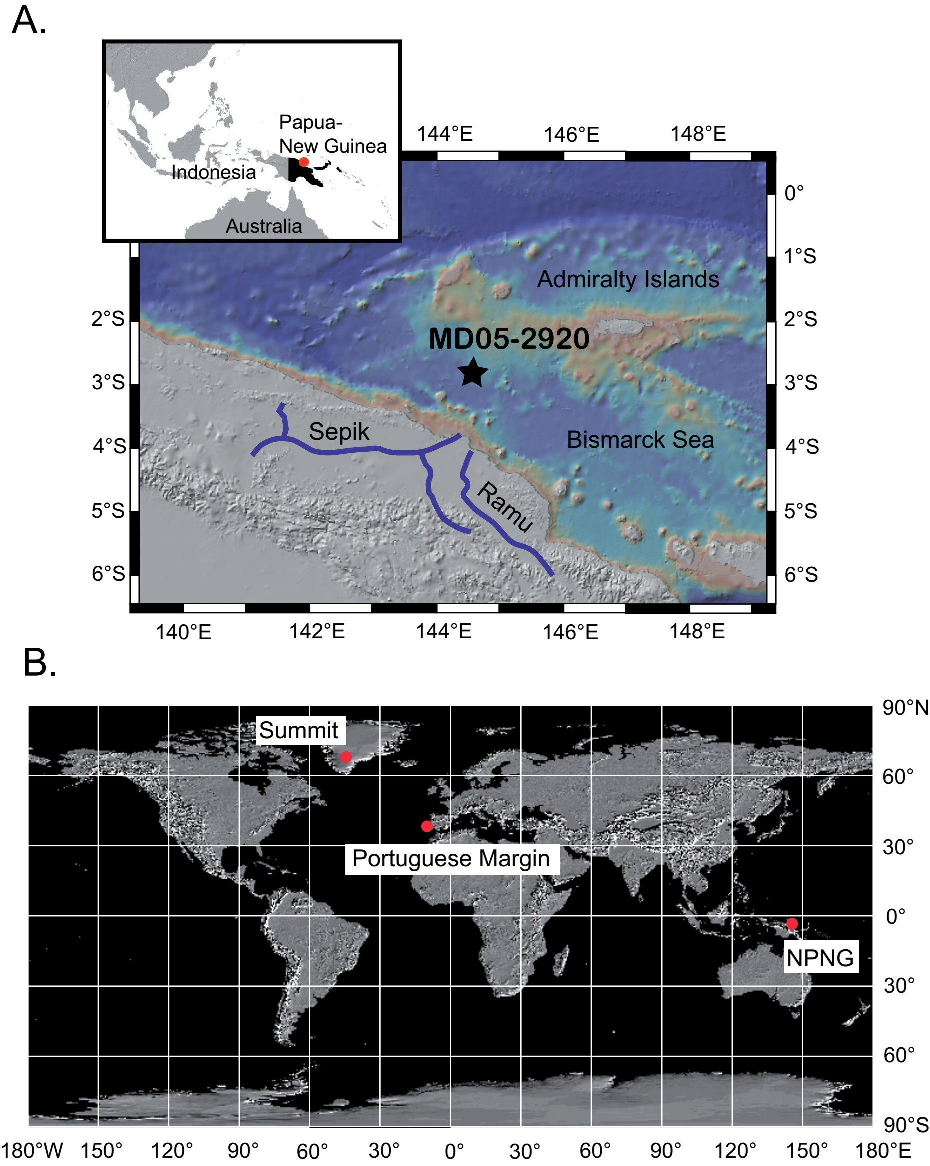
A.
Papua-
New Guinea
Indonesia
Australia
144°E
146°E
148°E
0°
1°S
2°S
3°S
4°S
5°S
6°S
Admiralty Islands
MD05-2920
Sepik
Ramu
Bismarck Sea
140°E
142°E
B.
Summit
Portuguese Margin
NPNG
90°N
60°
30°
0°
30°
60°
90°S
180°W
150°
120°
90°
60°
30°
0°
30°
60°
90°
120°
150°
180°E

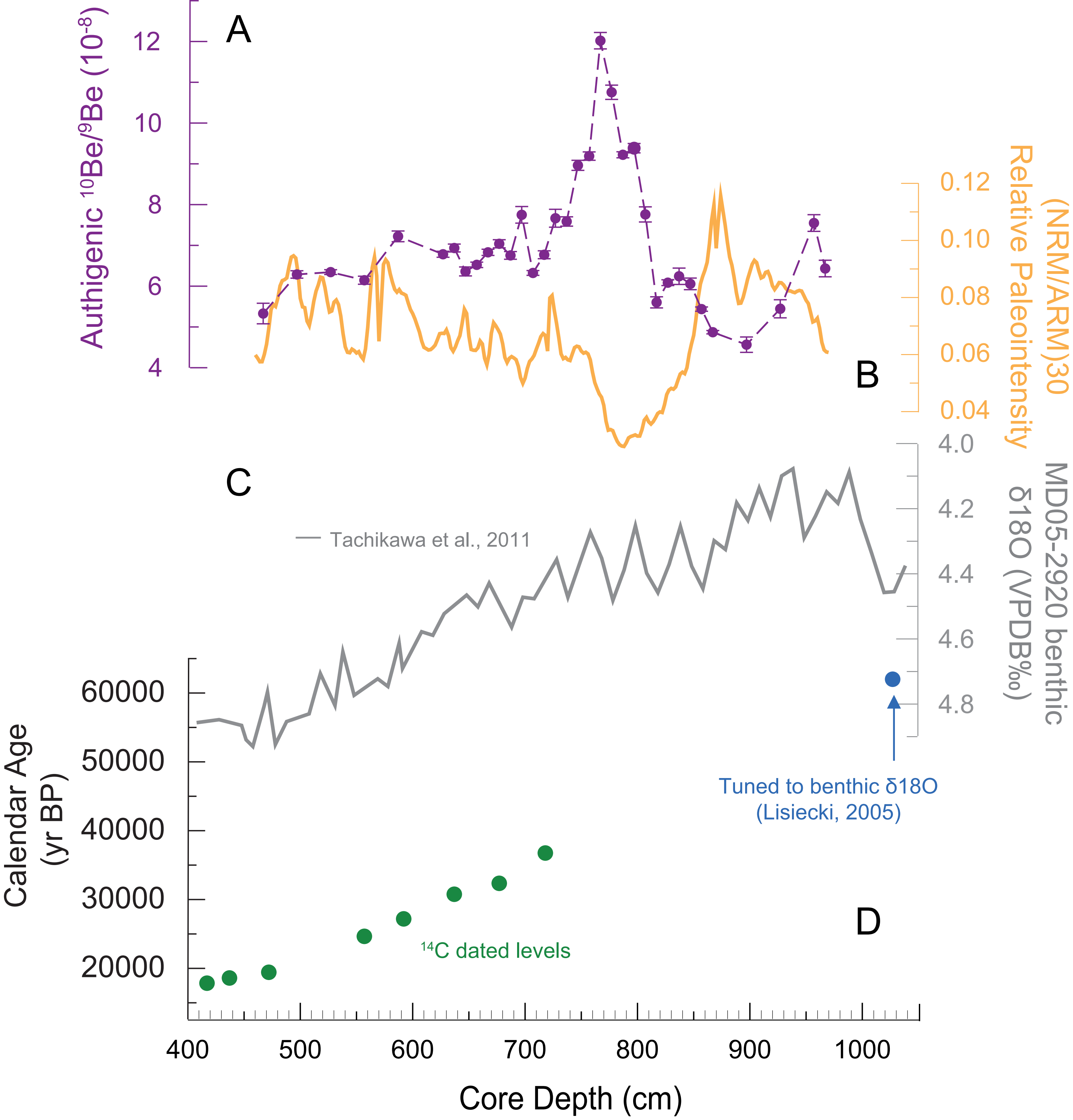
A
B
C
D
Authigenic $^{10}Be/^{9}Be$ (10^{-8})
12
10
8
6
4
(NRM/ARM)30
Relative Paleointensity
0.12
0.10
0.08
0.06
0.04
MD05-2920 benthic
δ18O (VPDB‰)
4.0
4.2
4.4
4.6
4.8
Tachikawa et al., 2011
Calendar Age
(yr BP)
60000
50000
40000
30000
20000
Tuned to benthic δ18O
(Lisiecki, 2005)
^{14}C dated levels
400
500
600
700
800
900
1000
Core Depth (cm)

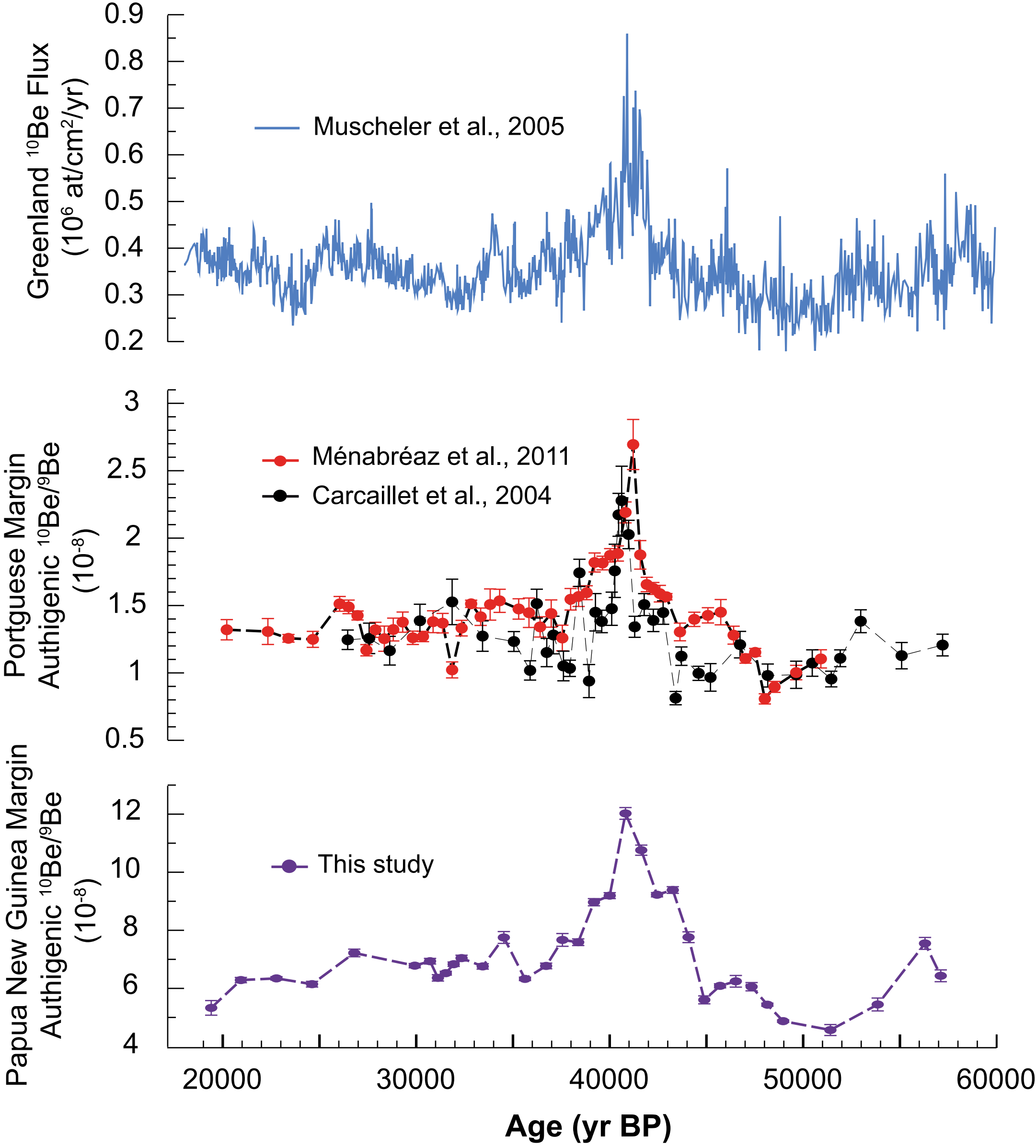

Greenland ^{10}Be Flux
(10^6 at/cm^2/yr)
Muscheler et al., 2005
0.9
0.8
0.7
0.6
0.5
0.4
0.3
0.2
Portguese Margin
Authigenic ^{10}Be/^{9}Be
(10^{-8})
Ménabréaz et al., 2011
Carcaillet et al., 2004
3
2.5
2
1.5
1
0.5
Papua New Guinea Margin
Authigenic ^{10}Be/^{9}Be
(10^{-8})
This study
12
10
8
6
4
20000
30000
40000
50000
60000
Age (yr BP)

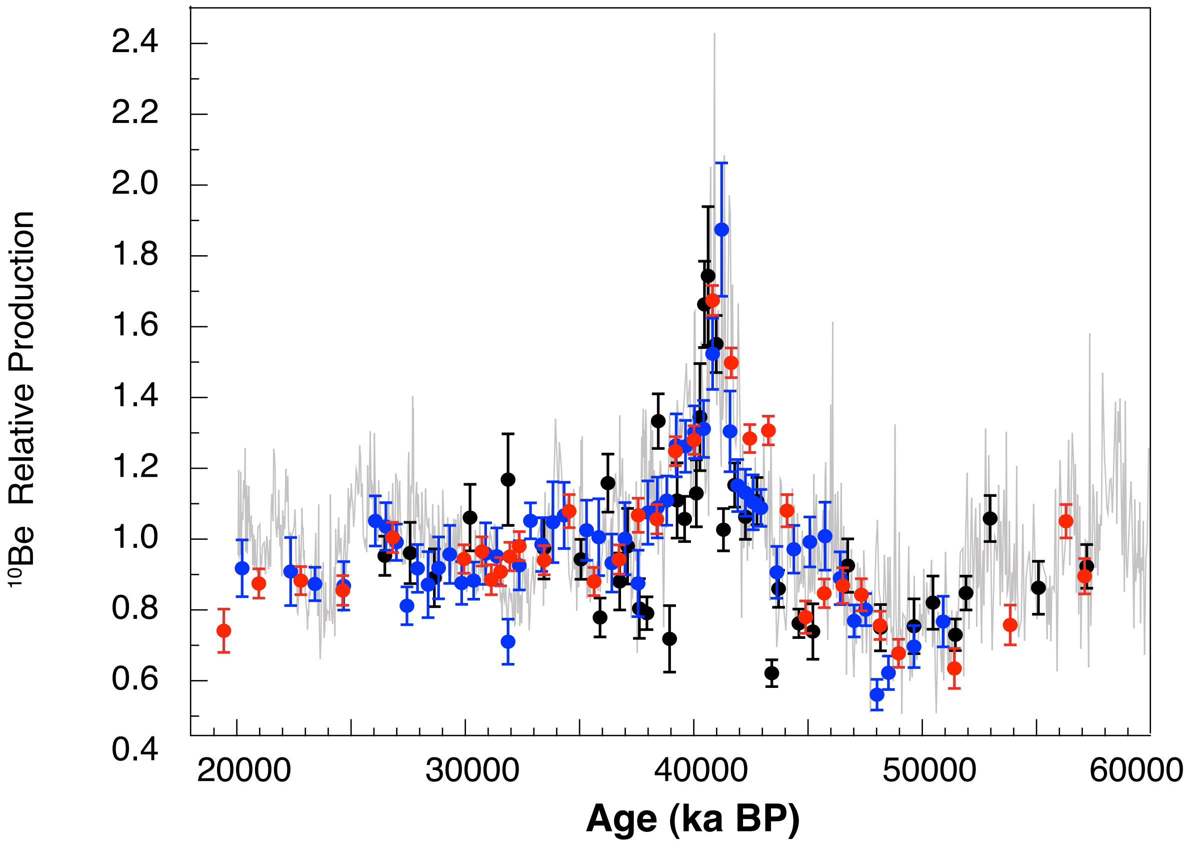

2.4
2.2
2.0
1.8
1.6
1.4
1.2
1.0
0.8
0.6
0.4
^{10}Be Relative Production
20000
30000
40000
50000
60000
Age (ka BP)

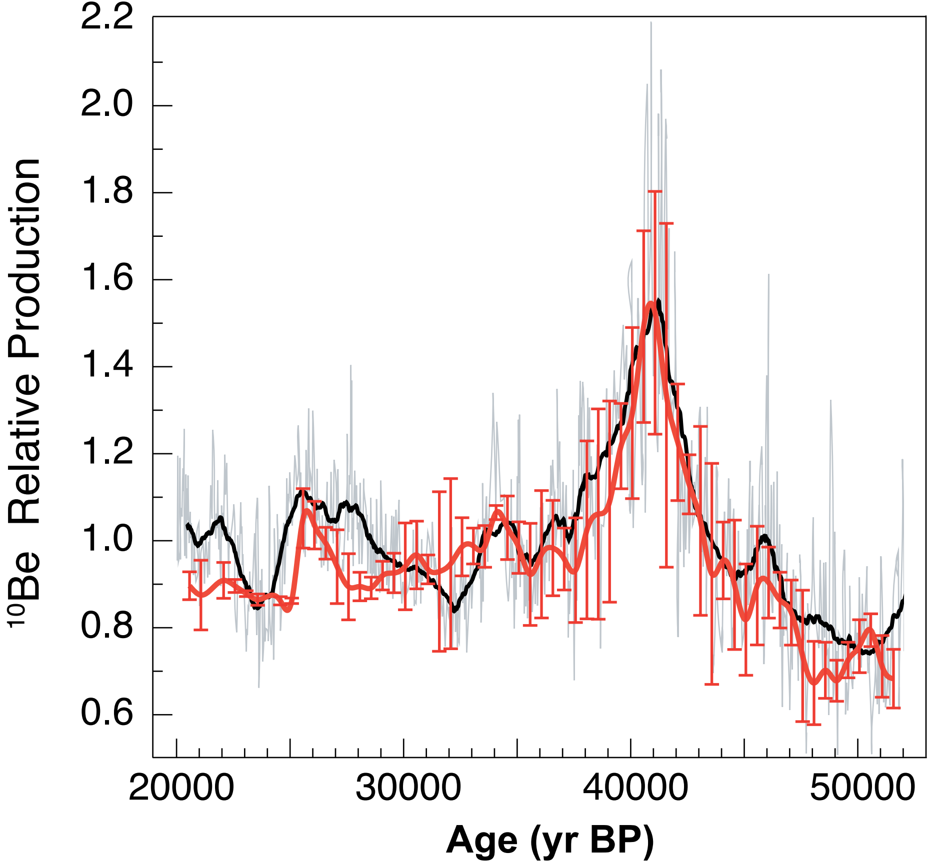

2.2
2.0
1.8
1.6
1.4
1.2
1.0
0.8
0.6
^{10}Be Relative Production
20000
30000
40000
50000
Age (yr BP)

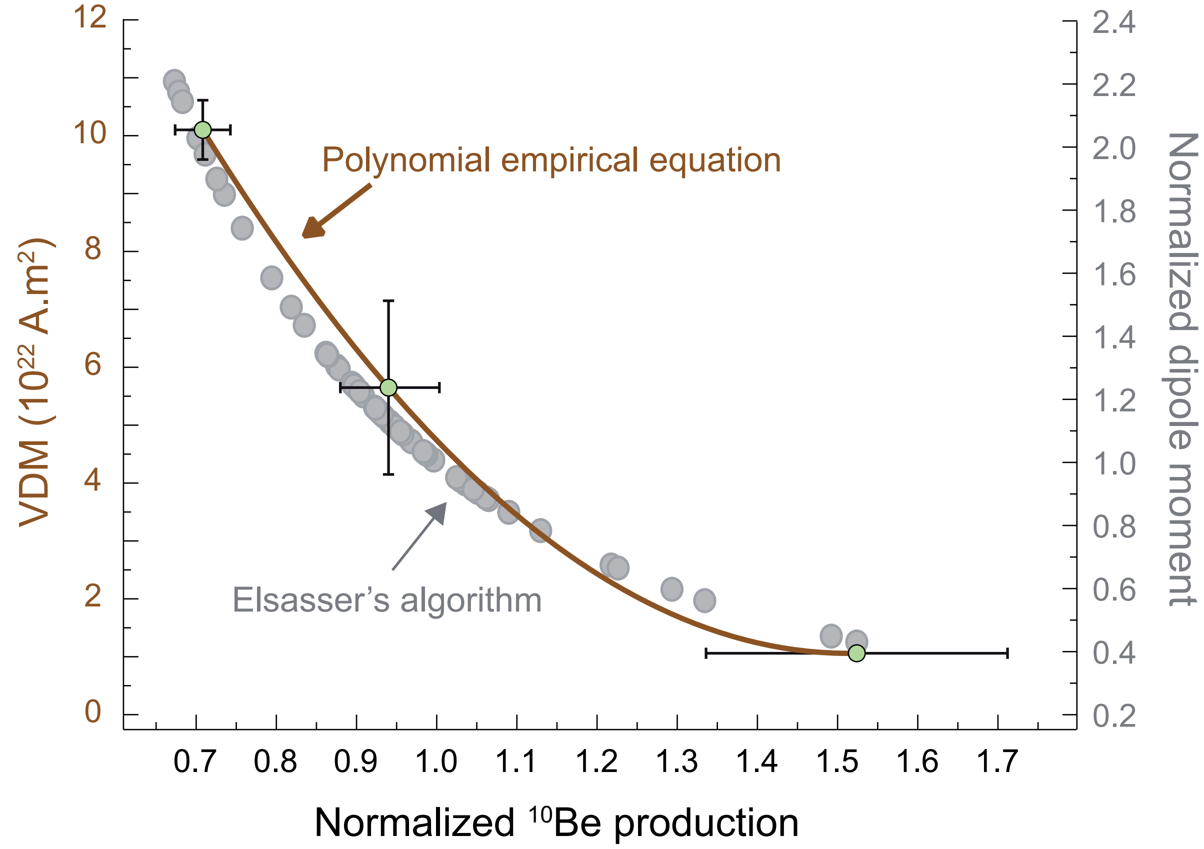

Polynomial empirical equation
Elsasser's algorithm
VDM (10^{22} A.m^2)
Normalized dipole moment
Normalized ^{10}Be production
0
2
4
6
8
10
12
0.2
0.4
0.6
0.8
1.0
1.2
1.4
1.6
1.8
2.0
2.2
2.4
0.7
0.8
0.9
1.0
1.1
1.2
1.3
1.4
1.5
1.6
1.7

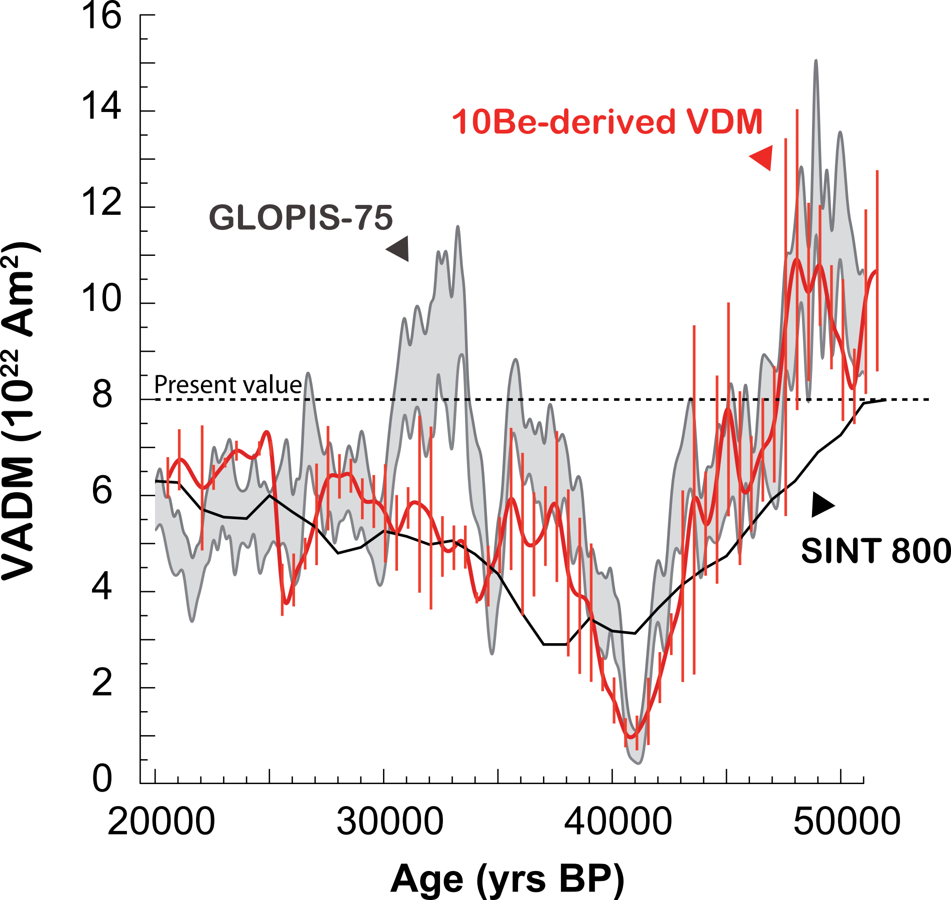
16
14
12
10
8
6
4
2
0
VADM (10^{22} Am^2)
10Be-derived VDM
GLOPIS-75
Present value
SINT 800
20000
30000
40000
50000
Age (yrs BP)

Table1: AMS measurements, Be isotopes concentrations and authigenic $^{10}Be/^{9}Be$ ratios of core MD05-2920 samples.

Sample: Core name-sample depth in core (cm)	Age (BP)	Measured $^{10}Be/^{9}Be$ (10^{-11}) *	Decay-corrected authigenic [^{10}Be] (10^{-14}g/g) *	Authigenic [^{9}Be] (10^{-7}g/g) *	Authigenic $^{10}Be/^{9}Be$ (10^{-8}) *
MD05 2920-467	19405	2.134±0.021	0.956±0.009	1.793±0.083	5.33±0.26
MD05 2920-797	20937	3.307±0.034	1.535±0.016	2.442±0.026	6.29±0.10
MD05 2920-527	22777	3.148±0.029	1.475±0.014	2.325±0.006	6.34±0.06
MD05 2920-557	24616	3.246±0.031	1.558±0.015	2.536±0.033	6.15±0.10
MD05 2920-587	26798	2.508±0.024	1.701±0.016	2.355±0.037	7.22±0.14
MD05 2920-627	29925	4.097±0.035	1.723±0.015	2.540±0.017	6.78±0.08
MD05 2920-637	30714	4.094±0.035	1.724±0.015	2.486±0.028	6.94±0.10
MD05 2920-647	31121	3.636±0.033	1.541±0.014	2.423±0.036	6.36±0.11
MD05 2920-657	31529	3.546±0.033	1.457±0.014	2.233±0.010	6.52±0.07
MD05 2920-667	31936	3.604±0.032	1.538±0.014	2.252±0.016	6.83±0.08
MD05 2920-677	32343	3.693±0.034	1.477±0.014	2.098±0.023	7.04±0.10
MD05 2920-687	33436	4.419±0.040	1.717±0.016	2.542±0.028	6.75±0.10
MD05 2920-697	34529	4.386±0.038	1.609±0.014	2.076±0.052	7.75±0.21
MD05 2920-707	35622	3.330±0.030	1.546±0.014	2.445±0.007	6.32±0.06
MD05 2920-717	36715	4.787±0.043	1.763±0.016	2.604±0.030	6.77±0.10
MD05 2920-727	37557	2.910±0.060	1.830±0.038	2.387±0.048	7.67±0.22
MD05 2920-737	38372	3.426±0.030	1.865±0.017	2.458±0.031	7.59±0.12
MD05 2920-747	39187	4.987±0.042	2.104±0.018	2.347±0.026	8.96±0.13
MD05 2920-757	40002	5.540±0.047	2.311±0.020	2.514±0.019	9.19±0.11
MD05 2920-767	40816	4.358±0.028	2.439±0.016	2.029±0.032	12.01±0.21
MD05 2920-777	41631	3.994±0.023	2.274±0.013	2.115±0.033	10.75±0.18
MD05 2920-787	42446	3.662±0.025	2.068±0.014	2.242±0.011	9.22±0.08
MD05 2920-797	43261	4.262±0.028	1.892±0.013	2.016±0.021	9.38±0.12
MD05 2920-807	44075	3.829±0.027	1.627±0.012	2.097±0.048	7.76±0.19
MD05 2920-817	44890	3.077±0.023	1.307±0.010	2.333±0.055	5.60±0.14
MD05 2920-827	45705	2.672±0.019	1.294±0.010	2.127±0.020	6.09±0.08
MD05 2920-837	46520	2.850±0.019	1.335±0.009	2.138±0.068	6.24±0.21
MD05 2920-847	47334	3.419±0.022	1.276±0.009	2.107±0.048	6.06±0.15
MD05 2920-857	48149	2.590±0.019	1.227±0.009	2.257±0.015	5.44±0.06
MD05 2920-867	48964	2.531±0.020	1.222±0.010	2.509±0.008	4.87±0.05
MD05 2920-897	51408	1.645±0.015	1.123±0.010	2.459±0.100	4.57±0.19
MD05 2920-927	53852	2.051±0.016	1.400±0.011	2.572±0.103	5.45±0.23
MD05 2920-957	56297	2.834±0.021	1.549±0.012	2.053±0.054	7.55±0.21
MD05 2920-967	57111	3.181±0.023	1.543±0.011	2.398±0.074	6.43±0.21
mean ± std. dev.			1.618±0.397	2.303±0.202	**7.07±1.62**
mean ± SDOM					**7.07±0.28**

* errors are 1 sigma, and rounded to the higher value. Sample depths are corrected from the 30 cm surface sediment void.

Table 2: *Chronological data for MD05-2920 age model construction.*

Sample depth in core MD05-2920 (cm) [a]	^{14}C Age [b] (^{14}C yr BP)	Calibrated Age (yr BP)	Method
40	2610 ± 35	2151 ± 206	^{14}C AMS ages, INTCAL09 *
80	4445 ± 35	4553 ± 271	^{14}C AMS ages, INTCAL09 *
119	6040 ± 40	6463 ± 191	^{14}C AMS ages, INTCAL09 *
198	8965 ± 45	9544 ± 251	^{14}C AMS ages, INTCAL09 *
253	10120 ± 35	11000 ± 252	^{14}C AMS ages, INTCAL09 *
302	11835 ± 45	13289 ± 196	^{14}C AMS ages, INTCAL09 *
322	12525 ± 40	13973 ± 267	^{14}C AMS ages, INTCAL09 *
352	12575 ± 45	14146 ± 396	^{14}C AMS ages, INTCAL09 *
417	15130 ± 60	18375 ± 130	^{14}C AMS ages, INTCAL09 *
437	15710 ± 60	19405 ± 197	^{14}C AMS ages, INTCAL09 *
472	16710 ± 60	19405 ± 197	^{14}C AMS ages, INTCAL09 *
557	21030 ± 90	24616 ± 409	^{14}C AMS ages, INTCAL09 *
592	22840 ± 90	27162 ± 609	^{14}C AMS ages, INTCAL09 *
637	26430 ± 130	30714 ± 557	^{14}C AMS ages, INTCAL09 *
677	28560 ± 160	32343 ± 715	^{14}C AMS ages, INTCAL09 *
718	32520 ± 240	36824 ± 623	^{14}C AMS ages, INTCAL09 *
1027		62000	Tuned to benthic $\delta^{18}O$ **

[a] All depths in core MD05-2920 are corrected for a top-core 30 cm void.

[b] All ^{14}C ages were determined by *Tachikawa et al.* [2011], and corrected for a regional reservoir age of 420 ± 60 years given by *McGregor et al.* [2008]. Errors are 2-sigma.

* *Reimer et al.* [2009]

** *Lisiecki and Raymo* [2005], *Tachikawa et al.* [2011].

Table 3: Authigenic $^{10}Be/^{9}Be$ marine stacked record, and corresponding ^{10}Be-based VDM record.

Age (BP)	Authigenic $^{10}Be/^{9}Be$ stack (normalized data)	VDM (10^{22} $A.m^2$)
20572	0.90 ± 0.03	6.4 ± 0.4
21072	0.87 ± 0.04	6.7 ± 0.6
22072	0.91 ± 0.10	6.2 ± 1.3
22572	0.90 ± 0.02	6.4 ± 0.3
23072	0.88 ± 0.01	6.7 ± 0.1
23572	0.86 ± 0.01	6.9 ± 0.2
24572	0.86 ± 0.01	7,0 ± 0.1
25072	0.86 ± 0.01	7,0 ± 0.1
25572	1.05 ± 0.07	4,0 ± 0.5
26072	1.04 ± 0.07	4.2 ± 0.6
26572	1.00 ± 0.04	4.8 ± 0.3
27072	0.94 ± 0.09	5.6 ± 1.1
27572	0.90 ± 0.08	6.4 ± 1.1
28072	0.89 ± 0.04	6.4 ± 0.5
28572	0.89 ± 0.02	6.4 ± 0.4
29072	0.92 ± 0.03	5.9 ± 0.4
29572	0.93 ± 0.04	5.9 ± 0.6
30072	0.94 ± 0.09	5.6 ± 1,0
30572	0.97 ± 0.07	5.2 ± 0.8
31072	0.93 ± 0.04	5.7 ± 0.4
31572	0.93 ± 0.15	5.8 ± 1.8
32072	0.95 ± 0.16	5.5 ± 1.9
32572	0.99 ± 0.06	4.9 ± 0.6
33072	0.99 ± 0.05	4.9 ± 0.5
33572	0.99 ± 0.04	4.9 ± 0.4
34072	1.06 ± 0.02	3.9 ± 0.1
34572	1.03 ± 0.08	4.3 ± 0.6

35072	0.98	±	0.06	5,0	±	0.6
35572	0.92	±	0.12	5.9	±	1.5
36072	0.97	±	0.16	5.2	±	1.7
36572	0.98	±	0.11	5,0	±	1.1
37072	0.96	±	0.07	5.4	±	0.8
37572	0.93	±	0.13	5.8	±	1.6
38072	1.02	±	0.20	4.4	±	1.7
38572	1.06	±	0.22	3.9	±	1.6
39072	1.09	±	0.22	3.6	±	1.4
39572	1.22	±	0.09	2.3	±	0.4
40072	1.29	±	0.18	1.7	±	0.5
40572	1.49	±	0.21	1.1	±	0.3
41072	1.52	±	0.26	1.1	±	0.4
41572	1.33	±	0.31	1.5	±	0.7
42072	1.23	±	0.15	2.2	±	0.5
42572	1.13	±	0.08	3.1	±	0.4
43072	1.05	±	0.25	4.2	±	2,0
43572	0.92	±	0.28	5.9	±	3.6
44072	0.95	±	0.10	5.4	±	1.1
44572	0.09	±	0.15	6.3	±	2.2
45072	0.82	±	0.12	7.8	±	2.2
45572	0.90	±	0.13	6.4	±	1.8
46072	0.90	±	0.07	6.2	±	1,0
46572	0.86	±	0.07	7,0	±	1.1
47072	0.83	±	0.07	7.5	±	1.2
47572	0.74	±	0.15	9.5	±	3.9
48072	0.67	±	0.10	10.9	±	3.1
48572	0.70	±	0.06	10.2	±	1.9
49072	0.68	±	0.04	10.8	±	1.3
49572	0.73	±	0.04	9.7	±	1.1
50072	0.76	±	0.06	9,0	±	1.5

50572	0.79	±	0.04	8.3	±	0.8
51072	0.71	±	0.07	10,0	±	1.9
51572	0.68	±	0.07	10.7	±	2.1

errors are 1-sigma